

39. Drob, D. P., Ground-based optical detection of atmospheric waves in the upper mesosphere and lower thermosphere. Ph D thesis, University of Michigan, Ann Arbor, MI, 1996.
40. Reisin, E. R. and Scheer, J., Vertical propagation of gravity waves determined from zenith observations of airglow. *Adv. Space Res.*, 2001, **27**(10), 1743–1748.
41. Reisin, E. R. and Scheer, J., Gravity wave activity in the mesopause region from airglow measurements at El Leoncito. *J. Atmos. Sol.–Terr. Phys.*, 2004, **66**, 655–661.
42. Taylor, M. J., Gardner, L. C. and Pendleton Jr, W. R., Long-period wave signatures in mesospheric OH meinel (6, 2) band intensity and rotational temperature at mid-latitudes. *Adv. Space Res.*, 2001, **27**, 1171–1179.
43. Lopez-Gonzalez, M. J. *et al.*, Tidal variations of O₂ atmospheric and OH (6-2) airglow and temperature at mid-latitude from SATI observations. *Ann. Geophys.*, 2005, **23**, 3579–3590.
44. Aushev, V. M., Lyahov, V. V., Lopez-Gonzalez, M. J., Shepherd, M. G. and Dryna, E. A., Solar eclipse of the 29 March 2006: results of the optical measurements by MORTI over Almaty (43.03°N, 76.58°E). *J. Atmos. Sol.–Terr. Phys.*, 2008, **70**, 1088–1101.
45. Offermann, D., Friedrich, V., Ross, P. and Zahn, U., Neutral gas composition measurements between 80 and 120 km. *Planet. Space Sci.*, 1981, **29**, 747–764.
46. Walterscheid, R. L. and Schubert, G., A dynamical–chemical model of fluctuations in the OH airglow driven by migrating tides, stationary tides and planetary waves. *J. Geophys. Res.*, 1995, **100**, 17443–17449.
47. Yee, J.-H., Crowley, G., Roble, R. G., Skinner, W. R., Burrage, M. D. and Hays, P. B., Global simulations and observations of O(¹S), O₂ and OH mesospheric nightglow emissions. *J. Geophys. Res.*, 1997, **102**, 949–968.
48. Hickey, M. P., Schubert, G. and Walterscheid, R. L., Gravity wave driven fluctuations in the O₂ atmospheric (0-1) nightglow from an extended, dissipative emission region. *J. Geophys. Res.*, 1993, **98**, 13717–13729.

ACKNOWLEDGEMENTS. This work was carried out with funds provided by the Ministry of Science and Technology, Government of India. We thank the Director, Indian Institute of Geomagnetism (IIG), Navi Mumbai for encouragement to carry out this work. The night airglow observations at Kolhapur were carried out under the scientific collaboration programme (MoU) between IIG and Shivaji University, Kolhapur. We also thank the anonymous reviewer for valuable suggestions that helped improve the manuscript.

Received 18 April 2014; revised accepted 5 January 2015

Dynamical model of daily CO concentration over Delhi: assessment of forecast potential

Jurismita Baruah and Prashant Goswami*

CSIR Fourth Paradigm Institute (Formerly C-MMACS), Belur Campus, Wind Tunnel Road, Bengaluru 560 037, India

Advance and accurate forecasts of air pollutant concentrations have many applications at different scales, from traffic planning to health advisories. However, such models need to incorporate local factors and must be validated against local observations for applicability. It has been shown earlier that a dynamical model successfully simulates, in forecast mode, the observed (CPCB, India) daily concentrations of SPM, RSPM, SO₂ and NO₂ over Delhi. The present work shows that the model skill is also significant in predicting CO. Together with our earlier results, the present work to the robustness and enhanced scope of dynamical forecast of air pollution.

Keywords: Air pollution, carbon monoxide, dynamical model, mesoscale forecast.

ACCURATE simulation of pollutant concentrations over an air basin is important for many applications like estimation of emission loads, overall health risk assessment and traffic planning¹. Air pollution model with sufficient skill can also be used to assess how pollutant levels would change in response to changes in emission rate². Worldwide there have been efforts to develop and validate such air pollution models at different scales. As the pollutant concentrations over an air basin like a mega city strongly depend on the local emission processes, an air pollution model needs to incorporate the relevant local processes in its formulation. In urban areas vehicle, industries, wind-blown dust and domestic appliances are recognized as major sources of air pollution. However, relative contributions of these sources vary from one location to another.

Delhi, as a growing mega city, has seen manifold increase in its industrial, vehicular as well as domestic emissions³. The growing emission has serious environmental and societal implications related to ecological unbalance and environmental degradation. In recent years, transportation systems are growing at an unprecedented rate. Mobile source emissions are the maximum contributors of carbon monoxide (CO) in Delhi^{4,5}. Literature analysis reveals that CO has emerged as the main pollutant in urban centres, amounting approximately to 90% contribution through the transport sector alone⁶. Thus, there is an urgent need to develop a dynamical model

*For correspondence. (e-mail: goswami@cmmacs.ernet.in)

Table 1. Data on total number of vehicles and emission rates

Year	Type of vehicle			
	Two wheeler	Diesel driven car	Petrol driven car	Heavy vehicles
2009	3,797,943	124,020	1,859,370	230,398
2010	4,055,229	131,722	2,013,680	251,252
2011	4,342,403	146,139	2,173,323	270,841
Emission rate (E_R ; g/km)	0.72	0.06	0.84	4.97

Source: Refs 19 and 20.

capable of simulating and forecasting CO concentrations at different scales.

It has been shown that a dynamical model incorporating details like idling time and number of vehicles as well contributions from natural sources, can successfully simulate daily suspended particulate matter (SPM) concentration over Delhi⁷. This model was then successfully extended to forecasting daily concentrations of respirable particulate matter (RSPM), sulphur dioxide (SO₂) and nitrogen dioxide (NO₂) over Delhi⁸. Further, the model was also validated over smaller locations like ITO (a major traffic intersection in Delhi) and other sites like Pune and Mumbai⁹ and was shown to have useful skill. Subsequently, it was shown that the model could be used in forecast mode, driven by the meteorological fields forecasted by an atmospheric general circulation model (GCM) for skillful forecasts of pollutant concentration over different locations¹⁰. However, these simulations and validations were primarily for the four pollutants: SPM, RSPM, SO₂ and NO₂; an important question is the ability of the model to simulate concentration of CO, a pollutant of significant environmental and societal importance.

Exposure to CO is associated with serious health effects. In metropolitan areas where population and traffic density are relatively high, motor vehicles and other combustion sources can emit sufficient CO to cause health effects in the general population and in high-risk group¹¹⁻¹⁵. The most important health effect associated with exposure to CO is that it inhibits the oxygen-carrying capacity of the blood to vital organs such as heart and brain. Inhaled CO combines with the oxygen-carrying haemoglobin of the blood and forms carboxyhaemoglobin (COHb), which can reduce the ability of blood to transport oxygen^{11,15,16}. CO is easily absorbed through the lungs¹⁷, which can lead to neurological damage and even death¹⁸.

The objective of the present study is to explore the skill of the model applied earlier over Delhi, in simulating daily values of CO over Delhi air basin. To assess the applicability of the model to simulate dynamics of CO, we employed the same formalism as in our earlier studies^{7,8}, using forecasts from an atmospheric mesoscale model to drive the air pollution model. The model has detail formulation of processes related to emission of pollutants

like the number of vehicles, type of vehicle, emission rate by each type of vehicle, average vehicle speed and idling time (Table 1)^{19,20}.

The formulations of the various terms in eq. (1) have been described in our earlier works^{7,8}. We define the contribution of vehicular exhaust (S_V) to a species as

$$S_V = \sum_{n_t=1}^{N_T} \sum_{n_v=1}^{N_V} r(t) \cdot n_v(n_t) \cdot E_R(n_t) \cdot T_E(n_t), \quad (1)$$

where N_T is the total number of types of vehicles, N_V the total number of vehicles of type n_t , $E_R(n_t)$ the average emission rate from a vehicle of type n_t and $T_E(n_t)$ is the effective emission in a day.

In eq. (1), $r(t)$ is a positive random number between 0.8 and 1 that represents (random) fluctuations in the traffic volume with time (day).

The effective duration of emission in a day is modelled as

$$T_E(n_t) = (d(n_t)/v_0) + T_I(n_t), \quad (2)$$

where $T_I(n_t)$ is the average idling time, $d(n_t)$ the average distance travelled by vehicles of type n_t (km) and v_0 is the average speed of the vehicle.

Both T_I and v_0 are assumed to depend on the total volume of traffic (total number of vehicles):

$$T_I(n_t) = T_{I\phi} \cdot (1 + a(n_t)), \quad T_I \geq 0, \quad (3)$$

$$v_0 = v_u \cdot (1 - b \cdot N_T \cdot N_V), \quad v_0 \geq 0, \quad (4)$$

where a , b and $T_{I\phi}$ are constants which are determined through calibration. Equations (3) and (4) assume that although in a metropolitan area like Delhi all vehicles would move with the same average speed (regulated by traffic control), the idling time changes based on the type of vehicle, with the smallest (largest) idling time for the lightest (heaviest) vehicle; the increase in the number of vehicles reduces the average speed below a free traffic speed v_u .

The mathematical representation of dynamics of a species as well as the sources and sinks are as described in our earlier work^{7,8}. The sources of species concentrations

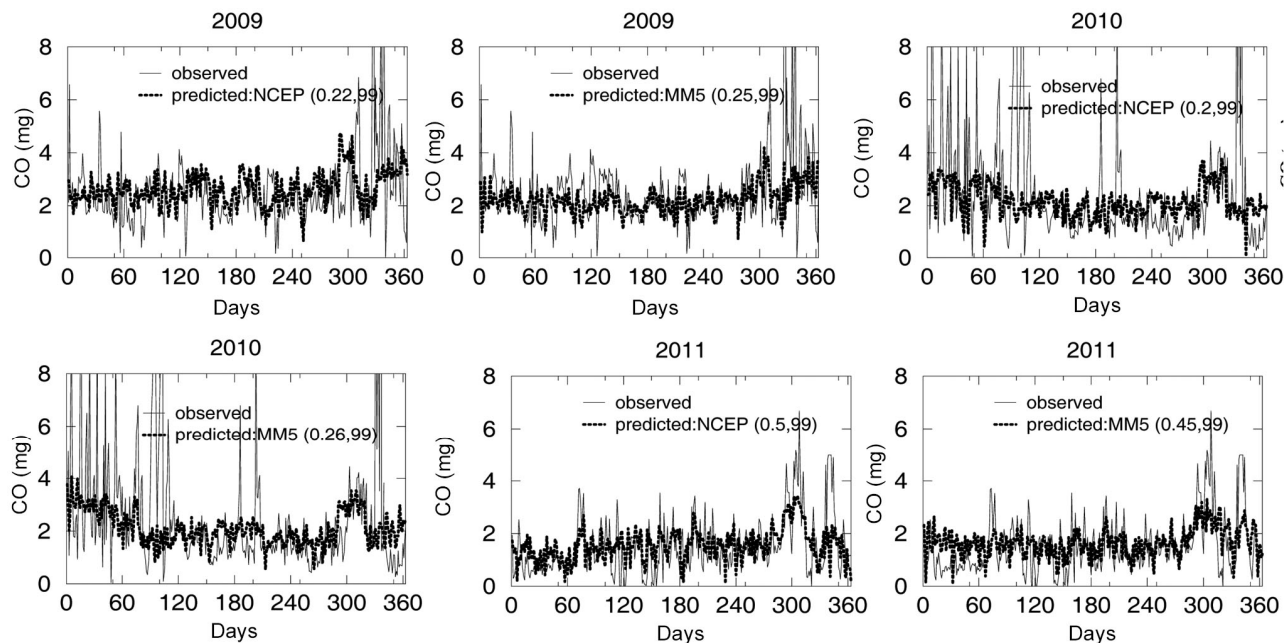


Figure 1. Daily values of CO over Delhi air basin from observation (CPCB, India) compared with simulation for the years 2009–2011. The left and the right panels indicate respectively, the simulations driven by NCEP and MM5-derived meteorological fields. The benchmark simulations with NCEP are based on area-averaged daily fields from NCEP Reanalysis (thick line) for the day of the forecast; the mesoscale forecasts (dotted line) are with lead of 24 h. The first number within brackets represents the correlation coefficient between observation and prediction; the second number represents the significance levels for corresponding correlation coefficients.

are vehicular exhaust (S_V) wind-blown dust (S_W) and domestic appliances (S_D). However, in the present study, we have neglected wind-blown dust as it is not known to contribute to the concentration of CO. The primary sinks of species are precipitation (S_P), removal due to advection (S_A) and dry deposition. The simulations are carried out for the period 2009–2011 for which CPCB observations on daily CO were available.

The daily atmospheric fields were taken from daily reanalysis of NCEP²¹ and a mesoscale atmospheric model (MM5). The configuration of MM5 model and values of the coefficients for static and dynamic sources used for NCEP fields as well as for MM5 model have been described in earlier studies⁹.

Based on samples of CO collected every 8 h throughout the day, CPCB compiles the data from its network by non-dispersive infrared spectroscopy method and provides daily values of pollutants. While the exact observational error statistics of the instruments used by CPCB is not available, we have used representative observational errors for non-dispersive infrared spectroscopy for our analysis. We have collected this observational error information from a report by US-EPA²². The number of vehicles (Table 1) was taken from data compiled by National Capital Territory of Delhi¹⁹ and the emission rates of CO for different vehicular types (Table 1) were adopted from data provided by Automotive Research Association of India²⁰.

The forecast skill is calculated by comparing daily forecasts generated by driving the air pollution model

with the meteorological fields from MM5 forecasts. As a benchmark for the skill, we consider daily CO concentrations calculated by driving the air pollution model with daily meteorological fields from NCEP Reanalysis averaged over Delhi for the day of the forecast. To evaluate the performance of the model, root mean square error (RMSE) was examined. RMSE (E_{RMSE}) is defined as

$$E_{RMSE} = \sqrt{\frac{\sum_{i=1}^n (P_i - O_i)^2}{n}},$$

where $n = 365$ and P_i and O_i are simulated and observed values of concentration on the i th day respectively.

Comparison of observed daily concentration of CO (CPCB) with the model simulations of CO for the years 2009–2011 (Figure 1) shows that the simulations with the two meteorological fields match the observed annual cycle well, although the model fails to capture some of the observed peaks, especially during the winter season. The performance of the model is reflected in the correlation coefficient greater than 0.2, above 95% confidence level for the degrees of freedom involved (Figure 1).

The daily observations and simulations averaged over 2009–2011 (Figure 2) show that the simulations capture the daily variability well, except for some persistent under-predictions in the winter months of November–December; it is likely that these indicate absence of some relevant seasonal sources in the model. In terms of seasonal

average (2009–2011), the winter maximum (5.52 mg) is followed by summer (2.08 mg) and monsoon (1.88 mg) in observation. The corresponding simulated values from NCEP and MM5 model-driven simulations are respectively, 4.34 and 4.60 mg in winter, 2.13 and 1.91 mg in summer and 1.85 and 1.80 mg during monsoon. Thus the seasonal variability in each case is well reproduced by the model; with improved winter simulation with mesoscale model. Another possible reason for this variability may be due to the meteorological conditions. The general meteorology over Delhi during winter is dominated by cold, dry air and ground-based inversion with low wind conditions, which facilitate stability of the atmosphere and thus more stagnant air masses. This can lead to accumulation of pollutants in a given area. As seen in our earlier studies^{7,8}, the winter maxima appear to be significantly controlled by domestic sources in case of SPM, RSPM, SO₂ and NO₂. During the summer months, the atmosphere is more conducive for the efficient dispersal of the pollutant as the average mixing height is typically at its maximum. This results in increased mixing processes through a greater volume of the troposphere, and hence lower

pollutant concentrations. The monsoon results in a large amount of precipitation, which reduces atmospheric pollution via associated wet deposition processes^{7,8}.

Scatter plots used for comparison of the observed and predicted values for the average over the three years show that the MM5 forecasts are better correlated with the observations than forecasts with NCEP (Figure 3). Predicted and observed CO concentrations are well correlated, with R^2 values 0.11 and 0.15 above 95% significance level. It was observed from the scatter plots that the CO concentrations are underestimated, particularly the peak values. The lines drawn over the scatters indicate best fit. An examination of year-wise values shows that the correlation is significant (Figure 4), indicating robust association between the observed and predicted values. In particular, for both the averages and the year-wise data, the results with MM5 forecasts are better correlated than those with NCEP Reanalysis (Figures 3 and 4).

While precise and accurate forecasts of pollutant concentration are useful, advisories can be issued if reliable forecasts of the level (category) of pollution were available. For a quantitative analysis of this skill, we have considered forecast errors as a fraction of the permissible value of CO concentration in a residential area (1 mg);

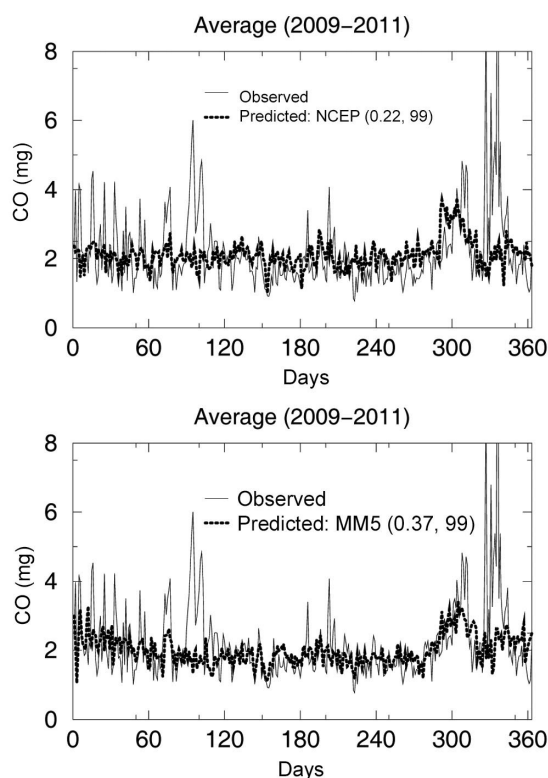


Figure 2. Average (2009–2011) CO over Delhi from observation (CPCB, India) compared with the simulation. The top and bottom panels indicate respectively, the simulations driven by NCEP and MM5-derived meteorological fields. The benchmark simulations with NCEP are based on area-averaged daily fields from NCEP Reanalysis (thick line) for the day of the forecast; the mesoscale forecasts are with lead of 24 h. The first number within the brackets represents the correlation coefficient between observation and prediction; the second number represents the significance levels for corresponding correlation coefficients.

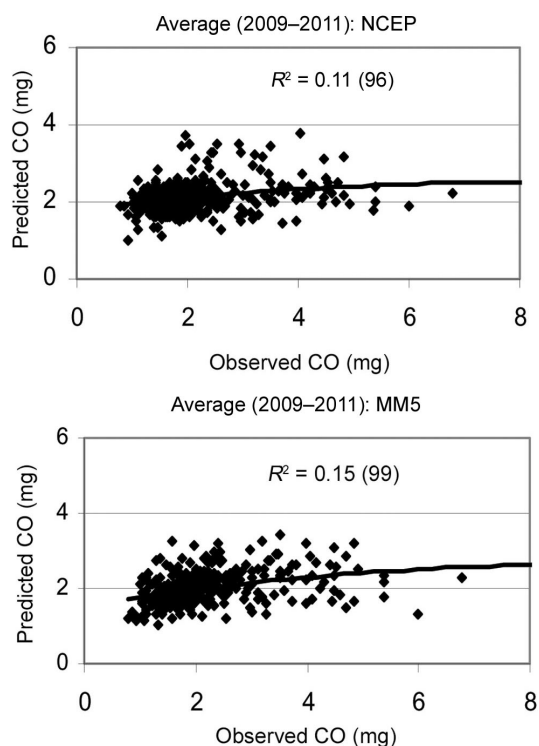


Figure 3. Scatter plots of average (2009–2011) of observed (CPCB, India) and predicted CO over Delhi. The top and bottom panels indicate respectively, the simulations driven by NCEP and MM5-derived meteorological fields. The benchmark simulations with NCEP are based on area-averaged daily fields from NCEP Reanalysis for the day of the forecast; the mesoscale forecasts are with lead of 24 h. Numbers within brackets provide the significance level for the corresponding R^2 values.

Table 2. Summary of performance

Parameter	2009			2010			2011			Average		
	Observed	NCEP	MM5									
Correlation coefficient	–	0.22	0.25	–	0.2	0.26	–	0.5	0.45	–	0.22	0.37
Number of days with error between -0.5 and $+0.5$ mg	–	142	174	–	126	135	–	174	180	–	189	226
Days >permissible level (1 mg)	338	267	296	291	217	241	253	295	279	345	294	300
Standard deviation (as percentage of observed mean)	57	23.1	20.3	52	24.6	25	60	40	35.6	56	25	40
No. of days with error less than observational error (0.5 mg)	–	117	142	–	124	124	–	184	190	–	131	150

The simulations with NCEP are based on area-averaged daily fields from NCEP Reanalysis for the day of the forecast; the mesoscale forecasts are with forecast lead of 24 h.

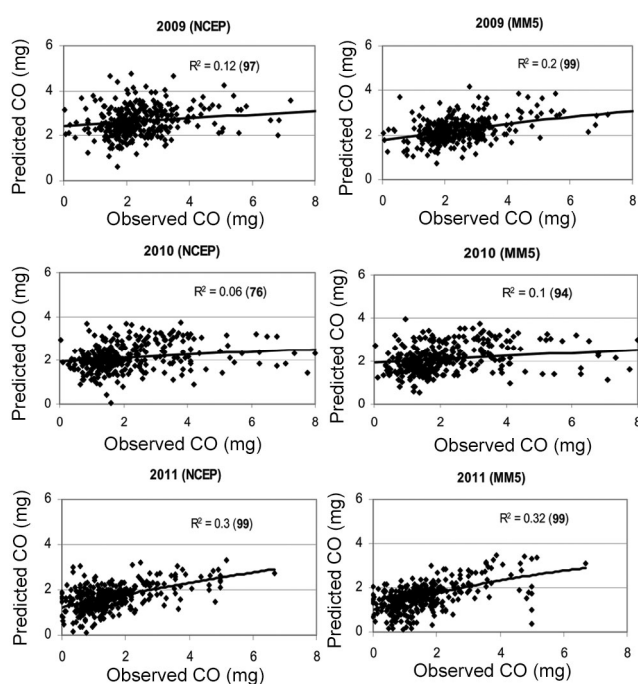


Figure 4. Scatter plots of observed (CPCB, India) and predicted CO over Delhi air basin for 2009–2011. The left and the right panels indicate respectively, the simulations driven by NCEP and MM5-derived meteorological fields. The benchmark simulations with NCEP are based on area-averaged daily fields from NCEP Reanalysis for the day of the forecast; the mesoscale forecasts are with lead of 24 h.

thus errors $\leq \pm 1$ indicate useful skill. An examination of the forecast skill in terms of the distribution of errors shows that the normalized error is between -1 and $+1$ for most of the days (Figure 5). The distributions of the number of days in different error bins (fraction of permissible value of CO) are almost Gaussian for all the cases; in particular, there is no appreciable systematic bias. While both simulations show comparable results, the mesoscale forecasts, in general, have higher number of days in the low-error bins. It may be seen that for the average of the three years, the number of days with error between -0.5 to $+0.5$ mg is 189 and 226 for the simulations with NCEP

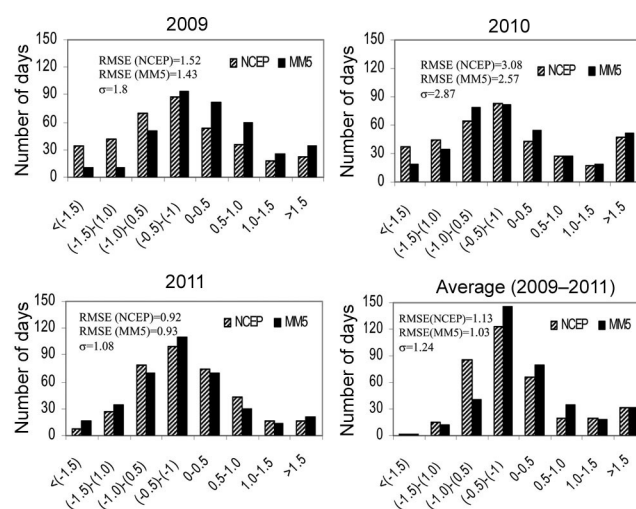


Figure 5. Histogram of errors showing the number of days in different error bins (observed–simulated) for the duration 2009–2011. The errors are expressed in terms of the permissible value of CO concentration over residential area. Standard deviation (σ) in the observed concentrations (daily values) for each year is given in the respective panel for comparison with the errors. The simulations with NCEP are based on area-averaged daily fields from NCEP Reanalysis for the day of the forecast and mesoscale (MM5) model. The observed data are from CPCB.

and MM5 respectively (Table 2). The evaluation of RMSE indicates that the simulation with NCEP for the year 2010 has much larger RMSE; in contrast, RMSE for all other cases is less than the standard deviation (σ) in the observed concentrations.

As another measure of the skill of the forecasts in terms of observational errors, we have considered forecast errors normalized to the precision of the instrument²² (0.5 mg). Histogram of the normalized errors once again shows that 65% of the days on average have normalized error <1 with MM5 forecasts; the corresponding number with NCEP Reanalysis is 54 (Figure 6, bottom right panel). This improvement with MM5 forecasts is also evident year-wise (Figure 6).

In terms of correlation coefficients between daily values of observed and simulated concentrations, the

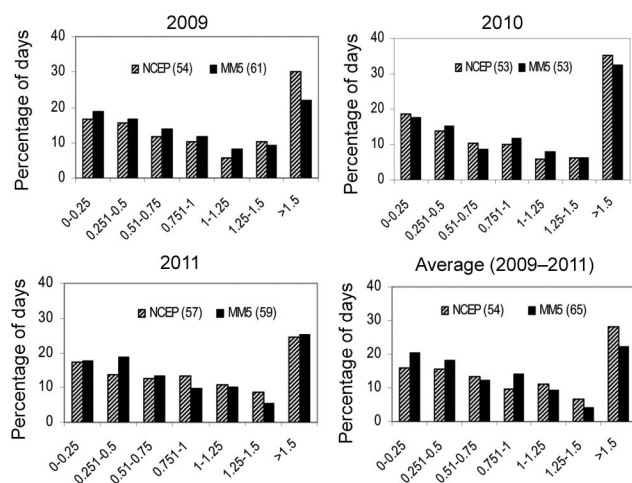


Figure 6. Histogram of errors in terms of number of days in different error bins for the duration 2009–2011. The errors (mg) have been normalized to a standard observational error (0.5 mg for non-dispersive infrared spectroscopy²²). Numbers within brackets indicate the percentage of days with normalized error <1.0. The simulations with NCEP are based on area-averaged daily fields from NCEP Reanalysis for the day of the forecast and mesoscale (MM5) model. The observed CO concentration data are from CPCB.

mesoscale forecasts improve the correlations, but only marginally (Table 2). However, in terms of application-relevant parameters like the number of days with CO concentration below permissible level, the mesoscale forecasts are closer to the observed values (Table 2). Similarly, the mesoscale forecasts provide more number of days in low-error bin (Table 2).

The present work provides an assessment of the ability of a dynamic air pollution model to simulate daily CO, validated against observations over Delhi. An accurate air pollution model also provides an effective tool for impact assessment for various uses. Together with our earlier results^{7–10}, the present work shows that comprehensive dynamical air pollution forecasting is feasible.

Comparison of air pollution forecasts with the mesoscale model and NCEP Reanalysis shows that the skill with mesoscale model is useful; extension to forecast at high spatio-temporal resolution will be useful for other applications like traffic management and health advisory.

1. SAEFL, La signification des valeurs limite d'immission de l'ordonnance sur la protection de l'air, Swiss Agency for the Environment, Forest and Landscape, Bern, 1992.
2. Dommen, J., Neftel, A. and Sigg, D. J., Jacob ozone and hydrogen peroxide during summer smog episodes over the Swiss plateau: measurements and model simulations. *J. Geophys. Res.*, 1995, **100**, 8953–8966.
3. Goyal, P., Mishra, D. and Kumar, A., Vehicular emission inventory of criteria pollutants in Delhi. *Springer Plus*, 2013, **2**, 216.
4. Mitra, A. P. and Sharma, C., Indian aerosols: present status. *Chemosphere*, 2002, **49**, 1175–1190.
5. Gurjar, B. R., Aardenne, J. A., Lelieveld, J. and Mohanb, M., Emission estimates and trends (1990–2000) for mega city Delhi and implications. *Atmos. Environ.*, 2004, **38**, 5663–5681.

6. Onursal, B. and Gautam, S., Vehicular air pollution: experiences from seven Latin American urban centers. World Bank Technical Paper No. 373, The International Bank of Reconstruction and Development, Washington DC, USA, 1997.
7. Goswami, P. and Baruah, J., Simulation of daily variation of suspended particulate matter over Delhi: relative roles of vehicular emission, dust and domestic appliances. *Mon. Weather Rev.*, 2008, **136**(9), 3597–3607.
8. Goswami, P. and Baruah, J., Urban air pollution: process identification, impact analysis and evaluation of forecast potential. *Meteorol. Atmos. Phys.*, 2010, **110**, 103–122.
9. Goswami, P. and Baruah, J., A comparative evaluation of a meso-scale model and atmospheric global circulation model for air quality simulation: a multi-scale, multi-site evaluation. *ISRN Meteorol.*, 2012, article ID 826074, p. 15.
10. Goswami, P. and Baruah, J., Urban air pollution: evaluation of forecast potential with GCM driven fields. *J Appl. Meteorol. Climate*, 2013, **52**(6), 1329–1347.
11. Varon, J., Marik, P. E., Fromm, R. E. and Gueler, A., Carbon monoxide poisoning: a review for clinicians. *J. Emergency Med.*, 1999, **17**, 87–93.
12. Aronow, W. S., Harris, C. N., Isbel, M. W., Rojaw, S. N. and Imparato, B., Effect of freeway travel on angina pectoris. *Ann. Intern. Med.*, 1972, **79**, 392–395.
13. Kurt, T. L., Mogielnicki, R. P. and Chandler, J. E., Association of the frequency of acute cardiorespiratory complaints with ambient levels of carbon monoxide. *Chest*, 1978, **74**, 10.
14. Godin, G., Wright, G. and Shephard, R. J., Urban exposure to carbon monoxide. *Arch. Environ. Health*, 1972, **25**, 305–313.
15. Von Burg, R., Toxicology update. *J. Appl. Toxicol.*, 1999, **19**, 379–386.
16. Maynard, R. L. and Waller, R., Carbon monoxide. In *Air Pollution and Health* (eds Holgate, S. T. et al.), Academic Press, Harcourt Brace & Company Publishers, 1999, pp. 749–796.
17. Ernst, A. and Zibrak, J. D., Carbon monoxide poisoning. *N. Engl. J. Med.*, 1998, **339**, 1603–1608.
18. Raub, J. A., Mathieu-Nolf, M., Hampson, N. B. and Thom, S. R., 'Carbon monoxide poisoning – a public health perspective'. *Toxicology*, 2000, **145**(1), 1–14; doi: 10.1016/S0300-483X(99)00217-6.
19. National Capital Territory of Delhi, Socio-economic profile of Delhi (2012–2013). A report prepared by Planning Department, Government of NCT of Delhi; Delhi Secretariat, New Delhi. www.delhiplanning.nic.in
20. Automotive Research Association of India, Air quality monitoring project – Indian Clean Air Programme (ICAP). Draft report on 'Emission factor development for Indian vehicles' as a part of ambient air quality monitoring and emission source apportionment studies, 2007.
21. Kalnay, E., Toth, Z., Tracton, S. M., Wobus, R. and Irwin, J., A synoptic evaluation of the NCEP ensemble. *Weather Forecast*, 1997, **12**, 140–153.
22. US Environmental Protection Agency, Air quality criteria for carbon monoxide. Office of Research and Development, National Centre for Environmental Assessment, Washington, DC 20460, EPA 600/P-99/001F, June 2000.

ACKNOWLEDGEMENT. This work was supported by a research grant under the Network project, 'Integrated Analysis for Impact, Mitigation and Sustainability', CSIR, New Delhi.

Received 29 April 2014; revised accepted 16 December 2014